Conductive Effect of an Electronic/Ionic Complex Conductivity Modifier for Silicone Elastomers

Hsien-Tang Chiu, Jyh-Horng Wu

Graduate School of Polymer Engineering, National Taiwan University of Science and Technology, Taipei, Taiwan

Received 2 October 2003; accepted 5 May 2004
DOI 10.1002/app.20978
Published online in Wiley InterScience (www.interscience.wiley.com).

ABSTRACT: This study examined silicone, which demonstrated an ionic/electronic compounding conductivity effect through the complexation of polypyrrole (Ppy), carbon black (CB), and a poly(propylene oxide)–poly(ethylene oxide) copolymer with 20 wt % $LiClO_4$ (PEL). Rigid-body pendulum rheometry was used to observe the processing conditions for the polymer blends, and energy-dispersive X-ray spectrometry was used to analyze the distribution depth of the polymer blend surfaces for Ppy. In addition, a digital electrometer was used to test the surface resistance of the composites, and an impedance meter was used to test the dielectric constant and loss factor. The results showed that PEL-obstructed silicone molecular chain crosslinking, transformed from liquid to solid films, required a higher temperature for curing than silicone because the linear molecular structure of the polymer electrolyte was wound around the silicone polymer network structure, forming a semi-interpenetrating network. This showed that the Ppy molecule could permeate SP10 blends more deeply. After the silicone was treated with the PEL modifier, the conductivity of Ppy was obstructed. On the other hand, the conductivity of CB showed no significant difference in the SP10 blends. Therefore, after the silicone matrix treatment of the electronic/ionic complex conduction process, there was no incremental effect on the conductivity. © 2005 Wiley Periodicals, Inc. J Appl Polym Sci 97: 711–720, 2005

Key words: polypyrroles; silicones; conductivity

INTRODUCTION

In recent years, the computer, communication, and consumer (3C) industries have moved toward the development of lighter weight, ultrathin, and short products. The connector is one of the essential parts of 3C products. The connector size and performance are constricted by the silicone insulation/conduction sandwich lamination structure. Therefore, fine insulation layers and silicone construction are the main issues in this project. Silicone is widely used in the electronics industry because it has extensive applications; the characteristics of silicon oxide are a low glass-transition temperature,[1,2] high impact resistance,[3,4] thermal stability,[5,6] high mechanical and chemical resistance, weather resistance, ozone resistance, and radiation resistance.[7,8] It is widely applied in various industrial products. It can compound with carbon black (CB),[9–14] carbon fibers, metal powders,[15,16] conducting polymers,[17–20] and polyelectrolytes[21] to conduct electricity.

Polypyrrole (Ppy) has been linked through the exchange of conjugate single bonds and double bonds and has been formed to be a fully conjugated aromatic polymer. Its electrical conductivity can reach up to 500 S cm^{-1}[22] under appropriate polymerization conditions with good stabilization[23,24] in air. The conductivity mechanism is in the region of the polymer chains. A poly(propylene oxide)–poly(ethylene oxide) copolymer with 20 wt % $LiClO_4$ (PEL) is one type of polymer electrolyte. It contains $LiClO_4$, which can move the lithium ion through the polymer chain to achieve ion conductivity. It can be applied to solid-state batteries, sensors, and display devices, among other things.

An electronic conduction mechanism governs Ppy and CB in polymer blends. On the other hand, an ion conduction mechanism governs PEL. This report shows that if the crystallization of the aggregate structure for the polymer matrix is high, it is beneficial to electronic conduction; if the crystallization is low, it is beneficial to ion conduction. On the other hand, the traditional conduction mechanism of a conduction filler for filling a polymer is explained by the percolation model. This implies that the electric conductivity of the matrix is an important parameter for the channel of electric conduction.

In this study, we tried to use the electronic conduction of CB and Ppy and the ionic conduction of PEL with a silicone matrix. The interaction between these two conduction mechanisms and the influence of the PEL modifier on silicone processing were evaluated.

EXPERIMENTAL

Materials

The materials were liquid silicone [poly(dimethylsiloxane); model 9050, Dow Corning] (Tokyo, Japan)

Correspondence to: H.-T. Chiu.

TABLE I
Compositions of the Silicone/PEL Blends with the PEL Concentration (wt %)

Material	Silicone	SP5	SP10	SP15	SP20
Silicone	100	95	90	85	80
PEL	—	5	10	15	20

and PEL (PEL-20A, Japan Carlit, Tokyo, Japan). The hardening agent was Coronate HX (Nippon Polyurethane Industry Co., Ltd., Tokyo, Japan). Pyrrole (Acros Organics, Geel, Belgium; 99%), an aqueous solution of acetonitrile [(CH_3CN); Osaka, Japan; 99%], the oxidizing agent ammonium peroxodisulfate [$(NH_4)_2S_2O_8$; Ferak, USA], Vulcan XC72 CB (Cabot Corp., Tokyo, Japan), and toluene ($C_6H_5CH_3$; Tedia, Fairfield, OH) were also used.

Sample preparation

The sample for testing was produced through the even mixing of silicone and PEL in accordance with the mixing proportions specified in Table I and through its placement in a mold. After being soaked *in vacuo* for 30 min, the mold was kept at 150°C for 30 min. Upon cooling, the test sample was removed from the mold and trimmed to the proper size for testing. In addition, the silicone and SP10 blends were added with 5–20 wt % CB and 200 mL of $C_6H_5CH_3$ through the application of agitators to every set of blends at room temperature at 300 rpm for 1 h, and the mold was maintained at 150°C for 30 min. In addition, the silicone and SP10 blends were in the B stage after the preheating process and were soaked in a 6*M* solution with CH_3CN for 10 min. The test sample was then removed and placed in a 0.1*M* $(NH_4)_2S_2O_8$ solution for 10 min. The dip-coating process was repeated four times. The test piece was coated with black, and an even Ppy membrane on the surface was obtained after curing at 150°C for 10 min.

Measurements

Principle of rigid-body pendulum rheometry (RPR)[25,26]

For a practical test of the curing process, the testing method made use of a damping pendulum system in compliance with the specifications of ISO 1522. To measure the curing process, a rigid-body pendulum equipped with a knife edge was provided. The test piece, coated or set on a plate, was placed on a heating mount, and the pendulum was set so that the edge, or the fulcrum of the swing, came vertically in contact with the coated surface (Fig. 1).

When an external force was applied by a magnetic adsorption force to the pendulum, the pendulum started to vibrate freely. Both sides of the edge of the pendulum yielded the strain of compression and elongation of the coated test piece. As a result, the viscoelastic property of the test pieces caused the swinging period of the pendulum and the swing damping action. Through the measurement of the logarithmic damping ratio (Δ), the curing behavior of the test piece could be obtained with the following equation (the change in the vibration wave during the curing process; Fig. 2):

$$\Delta = [\ln(A_1/A_2) + \ln(A_2/A_3) + \ldots \ln(A_n/A_{n+1})]/n$$

where A is the amplitude, and n is the number of the vibration wave.

The viscosity (η) of the substance had the function of stopping the oscillation of the oscillated body, which was in contact with the substance. Curing

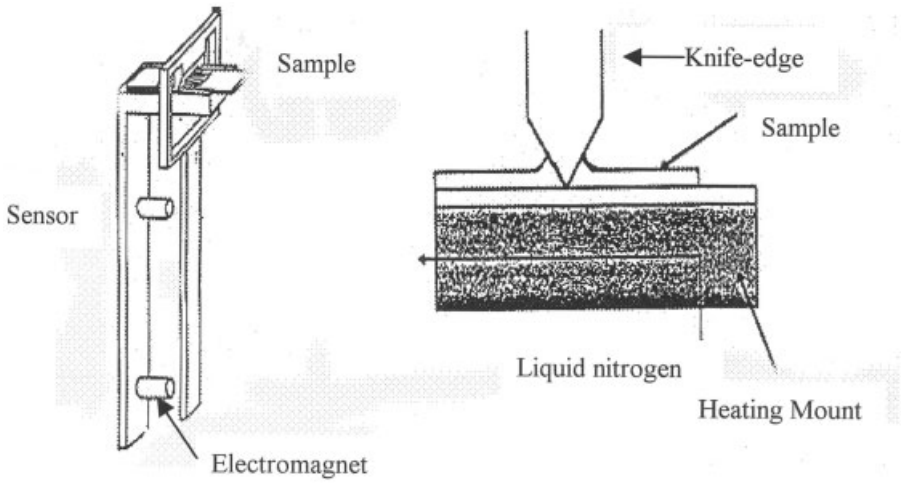

Figure 1 Instrument system.

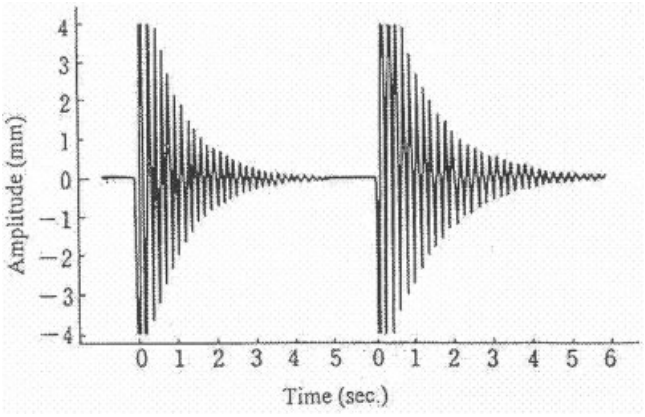

Figure 2 Changes in the vibration wave during the curing process.

changed the molecular weight (M). Therefore, as η became greater, the logarithm increased. η was evaluated with the following equations:

$$\eta = KM^{\theta}$$

$$\eta = ke^{\beta/t}$$

where t is the ambient temperature and k, θ, and β are constants.

Figure 3 shows the typical curing curve, as measured with the rigid-body pendulum instrument with theoretical analysis as follows. In curve C, the reaction begins after point 1, and M is increased; therefore, η increases as well. The increasing slope of η between points 3 and 4 shows the velocity of increased η. The first point of inflection is called the gel point, and its corresponding time is the gel time. After point 5, the last point of inflection is called the cure point, and its corresponding time is the cure time, which results in a balanced curve.

TABLE II
Curing Real Time of the Silicone/PEL Blends

	Temperature (°C)	Gel time (min)	Cure time (min)
Silicone	80	25	36
	100	10	15
	120	4	12
SP05	120	4	174
SP10	120	2	125
SP15	120	7	146

RPR measurements

A knife-edged, frame-type pendulum (RBE-130 and FRB-100) is an accessory of a rigid-body pendulum rheometer (Tohoku Electronic Industrial Co., Ltd., Tokyo, Japan).

Energy-dispersive X-ray spectrometry (EDS) analysis

A piece of the sample was examined with an energy-dispersive X-ray spectrometer (S-360, Cambridge Instrument, Cambridge, UK) to determine the weight percentage of nitrogen.

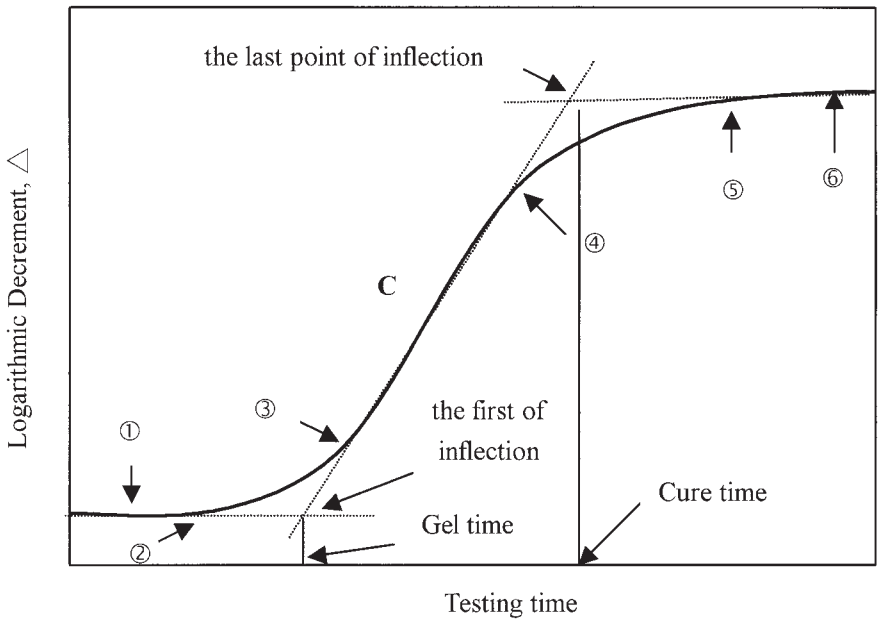

Figure 3 Curing behavior by RPR.

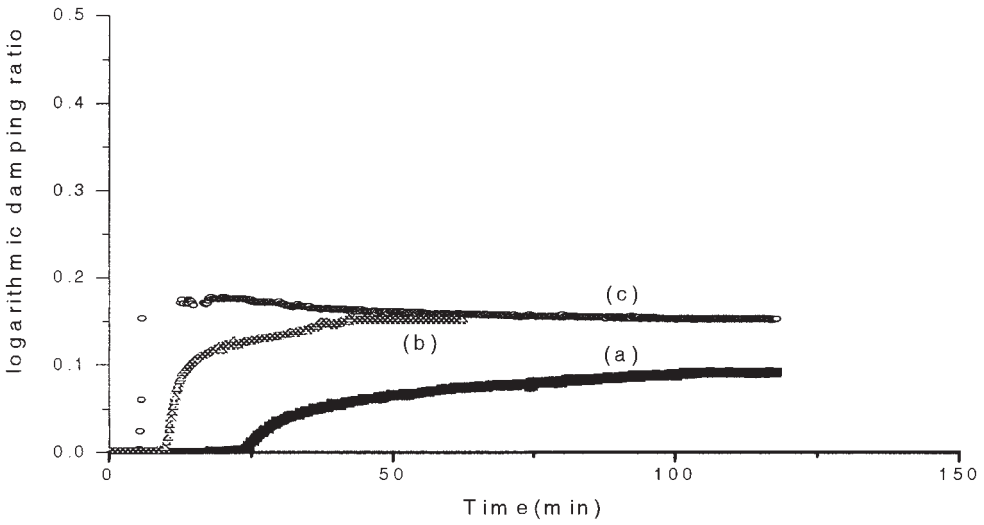

Figure 4 Curing process of silicone at (a) 60, (b) 80, and (c) 100°C.

Electronic/ionic conductivity measurements

Electrical/ionic conductivity measurements were taken with an Advantest TR8652 digital electrometer (Tokyo, Japan) at 25°C with a two-point probe technique.

Dielectric constant (E_r) and loss factor (tan δ) measurements

E_r and tan δ were measured with a Hewlett–Packard 4194A impedance meter (Tokyo, Japan) at frequencies between 0.5–15 MHz.

RESULTS AND DISCUSSION

Curing process of the silicone/PEL blends

Cone-and-plate rheometry is widely applied to the curing process of paints and photocuring resins. Because the curing process of materials is tested under the airtight conditions of the cone and plate, some paints with solvents and photocuring resins must be tested under open-room and illuminated environments. Thus, there are limitations to the use of cone-and-plate rheometry for testing the curing process for such materials. On the other hand, RPR tests the material curing process in an open environment. Therefore, RPR is suitable for testing the curing process of those paints with solvents and photocuring resins.

We used RPR in a thermostatic reaction system to observe the change in the properties for the blends of silicone/PEL during the curing process. The results after the gel time and curing time are shown in Table II. The curing curves of silicone under different curing temperatures are shown in Figure 4. According to the curing curve of silicone at 80°C, Δ is small during the

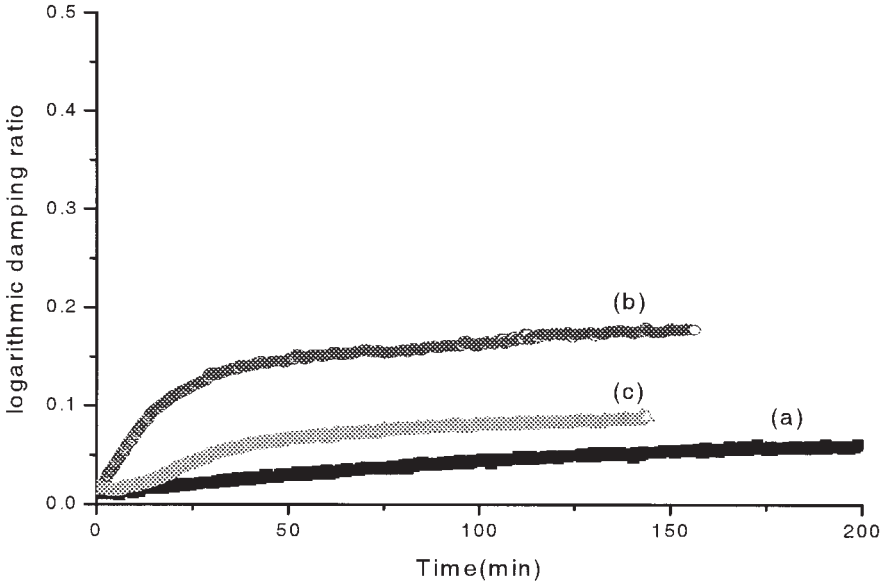

Figure 5 Curing process at 120°C: (a) SP05, (b) SP10, and (c) SP15.

TABLE III
EDS of the Permeate Depth of Ppy on Silicone and SP10 Blend Surfaces

	Permeate depth (μm)					
	5	7	10	150	200	300
Si-Ppyl	1.57[a]	3.17[a]	1.17[a]	—	—	—
SP10-Ppyl	21.36[a]	0.97[a]	9.10[a]	1.26[a]	2.82[a]	0.81

[a] Nitrogen content of permeate depth (wt %).

early stage of the curing process and starts to increase after about 25 min. This is the point at which the crosslinking starts. There is a transition on the Δ curve during the initial stage of the reaction, which is called the gel point, and the time corresponding to it is called the gel time. In about 36 min, the Δ curve becomes balanced during the transition process from liquid to solid films. When the curing temperature increases to 120°C, the silicone cures from liquid to solid (ca. 12 min), and the slope is maximum (the reaction rate is the speed) and coexists with the internal stress produced. At the end of curing, the internal stress disappears slowly with time, and the Δ relaxation balances. Thus, the curing time decreases as the curing temperature increases.

Figure 5 shows the curing curves of silicone with modified PEL (5–15 wt %). PEL-obstructed silicone molecular chain crosslinking transformed from liquid to solid films requires a higher temperature for curing than silicone. This phenomenon exists because the linear PEL polymer chain winds around the silicone network structure and disturbs the reaction of the crosslinking of the silicone molecular chain. Moreover, although the concentration of PEL is greater than 10 wt %, many lithium cations will complex easily with oxygen groups of silicone polymer chains because PEL contains the electrolyte of $Li^+ClO_4^-$. At this point, polymer chains will be tightly restrained by lithium cations. As a result, the curing rate and curing time will be slower than those of SP10 blends.

Permeate distribution of Ppy dip-coated on the silicone and SP10 blend surfaces

Ppy was dip-coated on the silicone and silicone/PEL surfaces, and the blends were under the B stage. During the process of curing, the molecular chain is fluid in the primary stage. This allows the pyrrole molecule to easily permeate the polyblend and the membranes of Ppy by *in situ* polymerization (chemical oxidation) on the blend surfaces of silicone and SP10. Table III shows elemental analyses of the Ppy permeates in silicone and SP10 blends. As the molecular structure of Ppy contains nitrogen atoms, EDS can test the concentrations of nitrogen in different locations of the blends. This number can be a reference for Ppy getting into the blends. From this diagram, we find that if the infiltrative depth of Ppy into the silicone blends is greater than 10 μm, the content of nitrogen atoms cannot be observed. After silicone is modified by PEL, we can observe for the blends the nitrogen atom content at the 300-μm infiltrative depth. Therefore, the result is better when Ppy permeates SP10 blends. The reason is that the silicone polymer is a crosslinked structure, whereas the PEL polymer is a linear structure. When these two are mixed with each other, the linear molecular structure of PEL is wound around the silicone polymer network structure, forming a semi-

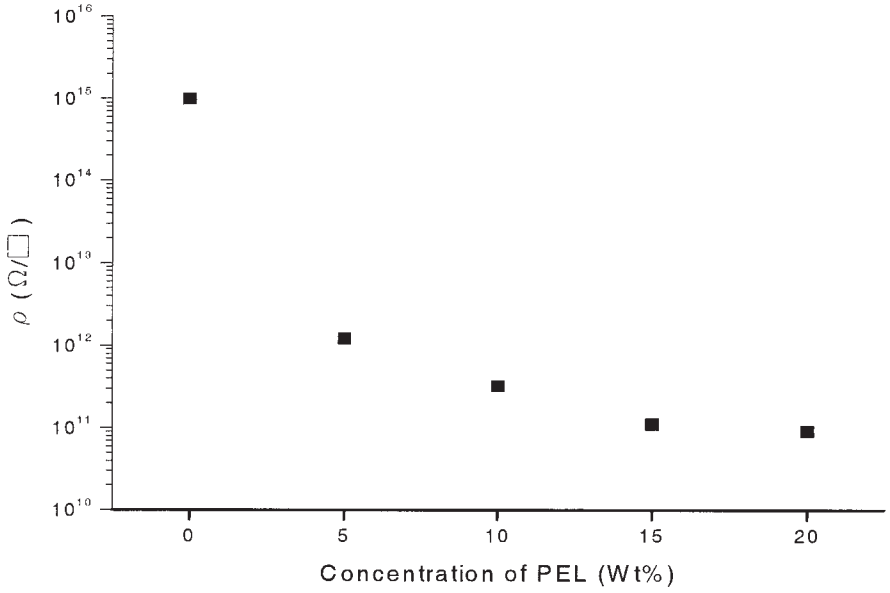

Figure 6 Surface resistance (ρ) of silicone/PELblends with the PEL concentration at 27°C.

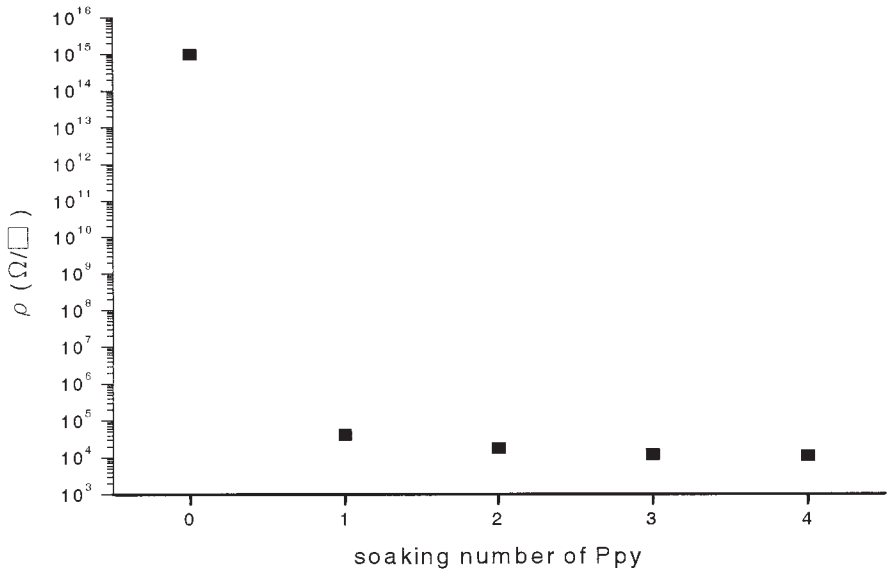

Figure 7 Surface resistance (ρ) of Ppy with the soaking number on silicone surfaces at 27°C.

interpenetrating network, which can reduce the density of the silicone crosslinked structure and influence the integrity of the crosslinked structure of the silicone. This allows the Ppy molecule to permeate easily inside the blends.

Ionic conductivity of the silicone/PEL blends

Figure 6 shows the surface resistance of silicone with different PEL concentrations at 27°C. The purpose of adding PEL was to enhance the ion electric conductivity. In the conductivity mechanism, lithium cations complex onto the sense base of a polymer chain and move the ion through the swinging of the polymer chain. When 5 wt % PEL is added to the silicone, the surface resistance of the silicone quickly decreases. When the concentration reaches 20 wt %, the decrease in the surface resistance of silicone is not obvious. To enhance the conductivity of silicone without destroying the characteristics, we have chosen blends with 10 wt % PEL as the matrix for the experiments.

Electronic/ionic conductivity of the silicone/PEL/Ppy composites

Figures 7 and 8 present curve diagrams of the resistance of Ppy coated onto the silicone surface for different times. The principle of electric conduction in the

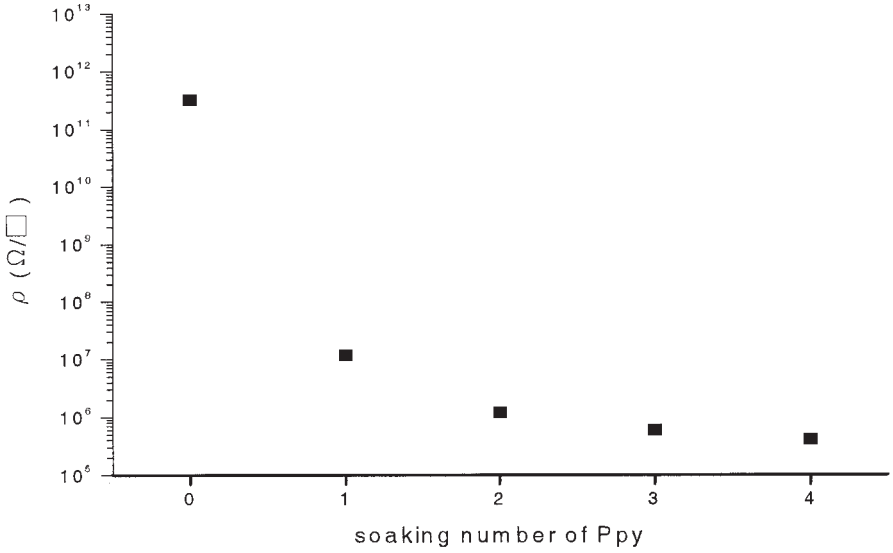

Figure 8 Surface resistance (ρ) of Ppy with the soaking number on SP10 surfaces at 27°C.

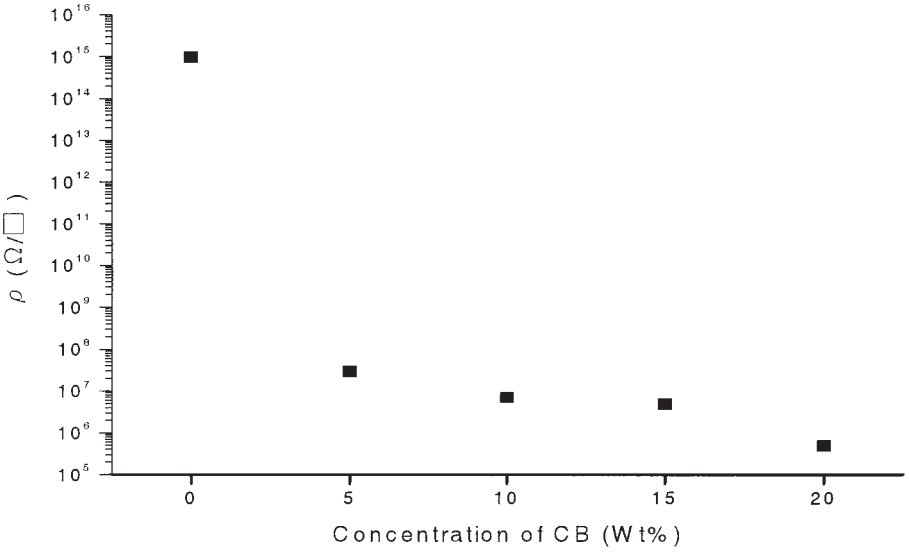

Figure 9 Surface resistance (ρ) of silicone with the CB concentration at 27°C.

blends of the Ppy membranes formed on the surfaces of the blends is to lead the pyrrole with heterocyclic molecules to the acceptor via doping and to make the pyrrole molecule structure transform into an electron-transfer complex. This increases the conduction and enhances the electric conductivity of the blends. Therefore, we know that the surface resistance decreases quickly when Ppy is coated onto silicone and SP10 blends. If this is done more than twice, no obvious change occurs. Moreover, SP10/Ppy possesses an ionic and electronic conductivity mechanism, yet the electric conductivity of a Ppy membrane on SP10 is worse than that of silicone. This tells us that the electric conductivity of Ppy occurs mainly on the molecular chain field in an ordered arrangement. The electric conductivity of PEL occurs on the amorphous field of the molecular chain. From the EDS results, we know that PEL influences the crosslinked structure of silicone. This allows the pyrrole molecule to permeate the silicone/PEL blends easily. Therefore, the restriction of the interaction between Ppy and SP10 molecular chains is more than others obstructing the electric conductivity of Ppy.

Electronic/ionic conductivity of the silicone/PEL/CB composites

Figures 9 and 10 shows surface resistance curves of silicone and SP10 blends at different CB concentrations. When the concentration of CB increases to 20 wt

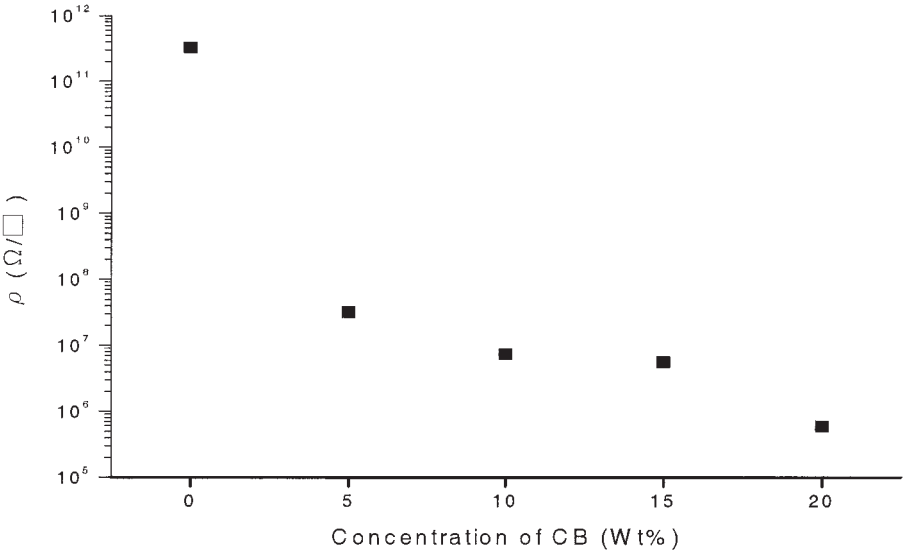

Figure 10 Surface resistance (ρ) of SP10 with the CB concentration at 27°C.

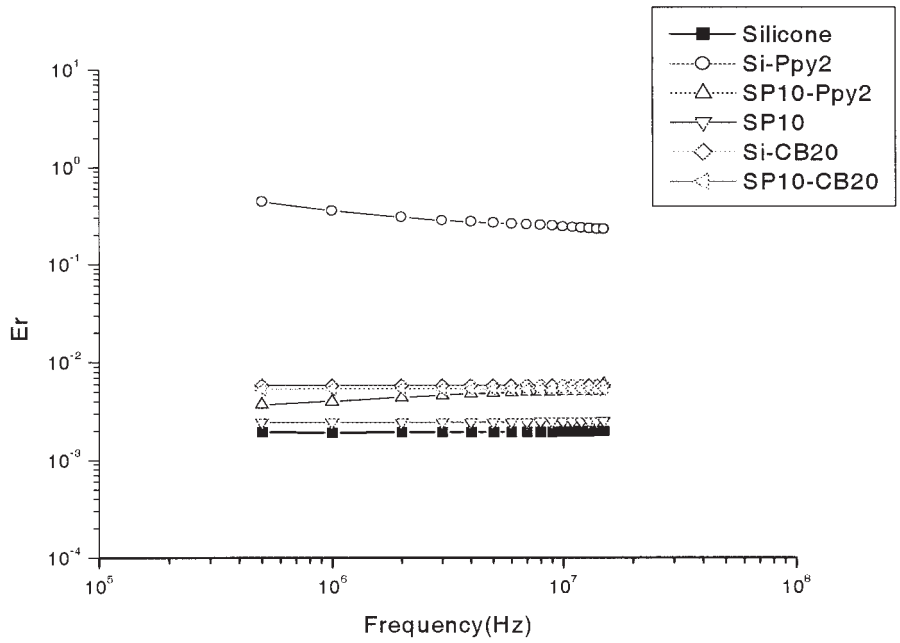

Figure 11 E_r versus the frequency.

%, the surface resistance reaches 5×10^5 Ω/□, where □ is equal to 1 cm^2. If 10 wt % PEL is added to silicone, there is no obvious difference in the surface resistance. Thus, we know that the conduction mechanism of silicone/PEL/CB is made through the aggregation of the CB particles, which form a channel that enables the electrical conductivity of the blend. The concentration and distribution of CB control the electric conductivity of the blend. Therefore, when silicone is made conducting by the addition of the conductive filler, its conductivity is not affected by the PEL polymer action. That is, when the silicone is processed with the method of ionic/electronic compound conductivity, there is no double effect in the improvement of the surface resistance.

E_r and tan δ of the silicone/PEL/Ppy and silicone/PEL/CB composites

Figures 11 and 12 show E_r and tan δ curves at 0.5–15 MHz for the blends. E_r and tan δ increase when silicone is led with conductive materials. When both ionic

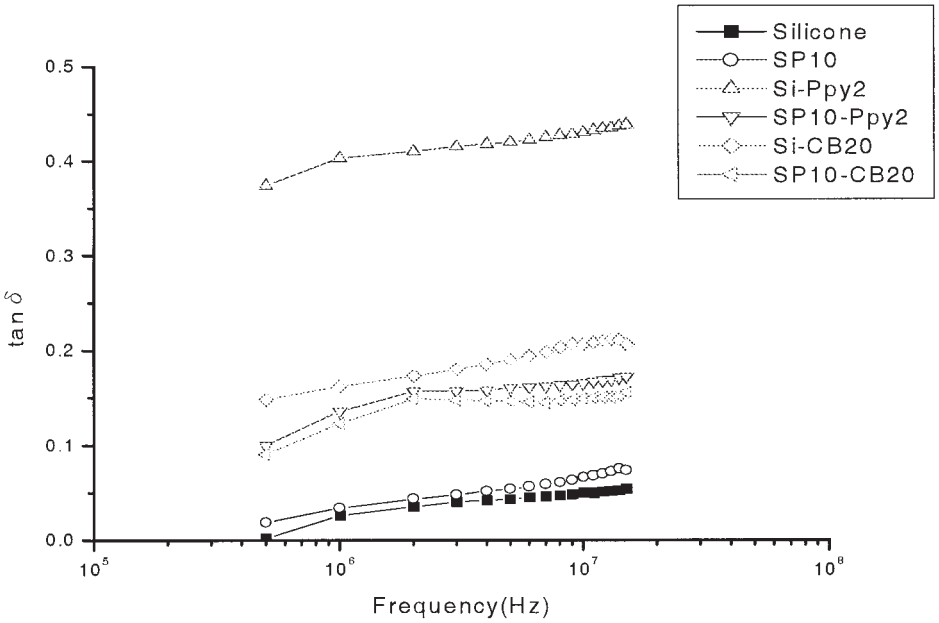

Figure 12 Tan δ versus the frequency.

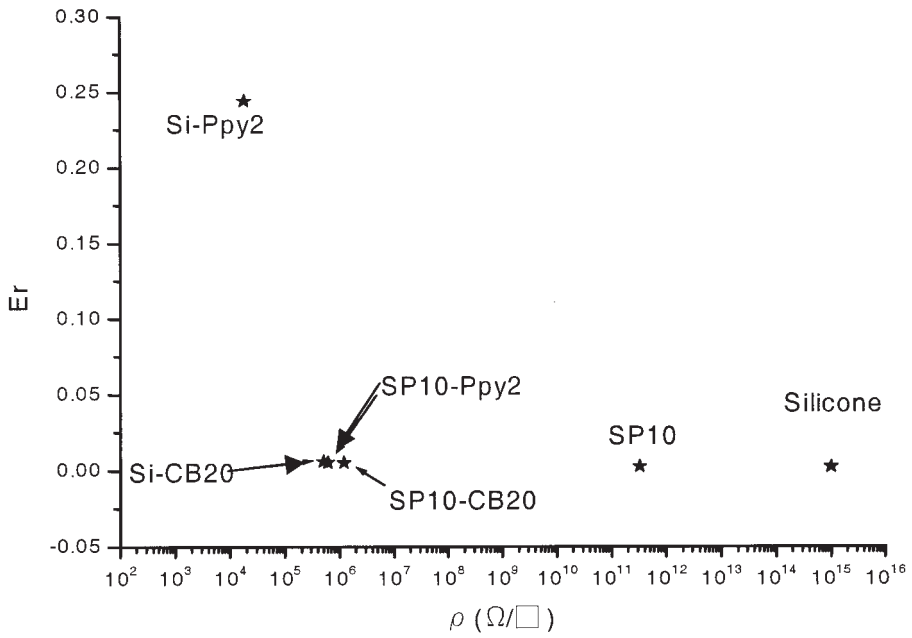

Figure 13 E_r/surface resistivity (ρ) responses at 10 MHz.

and electronic conductive materials are led with silicone blends at the same time, E_r and tan δ are worse than for materials with a single conducting mechanism. This phenomenon is the same as the result of the surface conductivity test of the blends. Figures 13 and 14 show the relationship between E_r, tan δ, and the surface resistance for each blend. When the surface resistance of the blends is lower, E_r and tan δ are larger. In addition, after the processing of the electronic/ionic complex conductivity of the blends, the improvement in E_r and tan δ is the same as its conductivity.

CONCLUSIONS

The following specific conclusion can be made from the experimental results:

1. RPR can be used to observe the change in the curing process for silicone/PEL blends. When the concentration of PEL is 10 wt %, the curing rate and curing time will be fastest.
2. The EDS analysis shows that PEL influences the integrity of the structure of the silicone network and allows the Ppy molecule to easily permeate the SP10 blends.

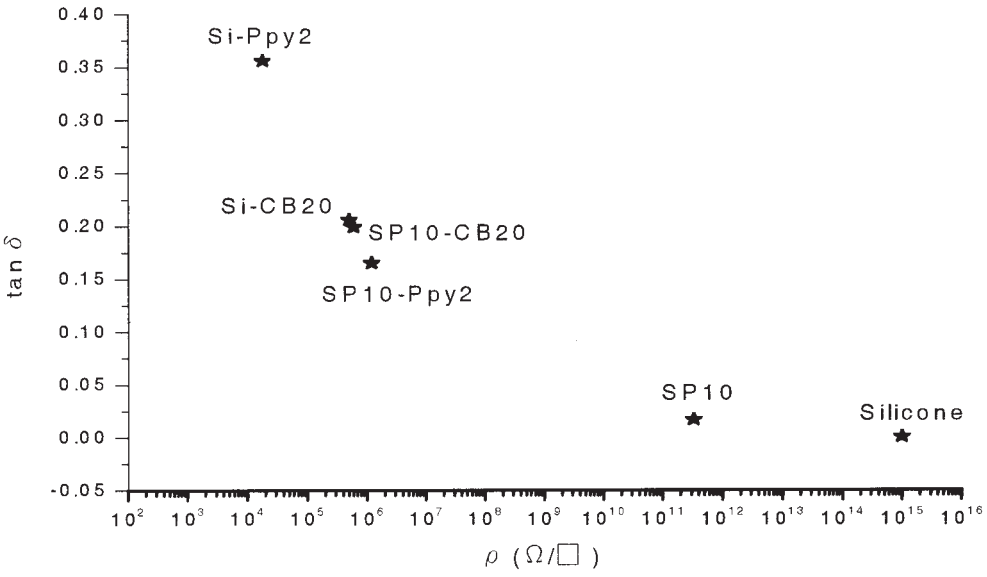

Figure 14 Tan δ/surface resistivity (ρ) responses at 10 MHz.

3. The surface resistance test shows that the surface resistance goes down after Ppy is coated onto the blend surface. The conductivity of Ppy is obstructed because the interaction of the silicone/PEL blend and the conductivity conflict between the ionic and electronic, limiting the Ppy conductivity.
4. After CB is added to the silicone matrix and the matrix is made conductive, the conductivity is controlled by the concentration and distribution of CB. Thus, the conductivity is not affected by an amorphous modifier.
5. After the electronic/ionic complex conduction process, there is no double effect on the conductivity for silicone. The lower the blend's surface resistance is, the larger E_r and tan δ are.

References

1. Ohiberg, S. M.; Alexander, L. E.; Warrick, E. L. J Polym Sci 1958, 27, 1.
2. Polmantee, K. E.; Hunter, M. J. J Appl Polym Sci 1959, 1, 3.
3. Hagerman, E. M. J Appl Polym Sci 1969, 13, 1873.
4. Matsuo, M.; Kondo, Y. Polym Eng Sci 1970, 10, 253.
5. Polmanteer, K. E. Rubber Chem Technol 1981, 54, 1051.
6. Yin, W. S.; Liu, H. W.; Gan, L. H. J Appl Polym Sci 1999, 72, 95.
7. Eaborn, C. Organosilicon Compound; Butterworths: London, 1962; p 100.
8. Noll, W. Chemistry and Technology of Siloxanes; Academic: New York, 1968; p 17.
9. Tamai, T. IEEE Transactions on Components, Hybrids and Manufacturing Technology, 1981, 5, 56.
10. Stern, H. Electron Packaging Prod 1980, 20, 237.
11. Kost, J.; Narkis, M.; Foux, A. Polym Eng Sci 1983, 23, 567.
12. Kost, J.; Narkis, M.; Foux, A. J Appl Polym Sci 1984, 29, 3937.
13. Kost, J.; Narkis, M.; Foux, A. Polym Eng Sci 1994, 34, 1628.
14. Poole, D. R. Plast Eng 1978, 34, 25.
15. Wang, X.; Yoshimura, N. J Appl Phys 1999, 38, 5170.
16. Lu, X.; Xu, G.; Hofstra, P. G.; Bajcar, R. C. J Polym Sci Part B: Polym Phys 1998, 36, 2259.
17. Gan, L. H.; Gan, Y. Y.; Yin, W. S. Polymer 1999, 40, 4035.
18. Tuyen, L. T. T.; Potje-Kamloth, K.; Liess, H. D. Thin Solid Films 1997, 292, 293.
19. Kim, N. Y.; Laibinis, P. E. J Am Chem Soc 1999, 121, 7162.
20. Lee, H. S.; Yan, X. Q.; Xiang, C.; McBreen, J.; Callahan, J. H.; Choi, L. S. J Electrochem Soc 1999, 146, 941.
21. Killis, A.; Cheradame, H.; Gandini, A.; Lenest, J. F.; Cohen, J. P. Solid State Ionics 1984, 14, 231.
22. Satoh, M.; Kaneto, K.; Yoshino, K. Synth Met 1986, 14, 289.
23. Diaz, A. F.; Kanazawa, K. K. J Chem Soc Chem Commun 1979, 14, 635.
24. Diaz, A. F.; Hall, B. IBM J Res Dev 1983, 27, 342.
25. Tanaka, T. Coating Films: Evaluation of Physical Properties; Ricogaka: Japan, 1993.
26. Tanaka, T. Proceedings of the International Pressure Sensitive Adhesive Technoforum; Tokyo, 1997.